



Learning-Induced Synchronization and Plasticity of a Developing Neural Network

T.-C. CHAO AND C.-M. CHEN*

Department of Physics, National Taiwan Normal University, Taipei, Taiwan
cchen@phy.ntnu.edu.tw

Received September 24, 2004; Revised May 17, 2005; Accepted May 31, 2005

Action Editor: Alain Destexhe

Published online: 28 October 2005

Abstract. Learning-induced synchronization of a neural network at various developing stages is studied by computer simulations using a pulse-coupled neural network model in which the neuronal activity is simulated by a one-dimensional map. Two types of Hebbian plasticity rules are investigated and their differences are compared. For both models, our simulations show a logarithmic increase in the synchronous firing frequency of the network with the culturing time of the neural network. This result is consistent with recent experimental observations. To investigate how to control the synchronization behavior of a neural network after learning, we compare the occurrence of synchronization for four networks with different designed patterns under the influence of an external signal. The effect of such a signal on the network activity highly depends on the number of connections between neurons. We discuss the synaptic plasticity and enhancement effects for a random network after learning at various developing stages.

Keywords: neural network, synchronization, plasticity

1. Introduction

The functions of the nervous system crucially rely on the synaptic connections among neurons. Studies on lower mammals have demonstrated that, in almost all peripheral and central nervous systems studied so far, synapses between neurons are established from the early developmental stages and activity-driven synchronization of neurons may occur during development and learning (Markram et al., 1998; Ben-Ari, 2001). It has been shown that immature pyramidal neurons of the rat hippocampus start to receive sequentially established synaptic inputs around birth (Tyzio et al., 1999) and the hippocampal network generates periodic

synchronized neuronal discharges during the first two postnatal weeks (Ben-Ari et al., 1989). Such a synchronized activity drives synchronized oscillations of intracellular calcium and provides conditions for Hebbian plasticity in developing synapses. Recent experimental advances, including real-time imaging of living neurons, have provided physical insight into the molecular and cellular processes that guide synaptogenesis in the developing nervous systems (Engert and Bonhoeffer, 1999; Ahmari et al., 2000; Jontes et al., 2000). Based on physically modeling experimental observations, computer assisted simulations can be very helpful in understanding the synchronized activities in a developing neural network and how the synaptic plasticity of the network is affected by learning. Furthermore, computer simulations can be complementary to experiments

*To whom correspondence should be addressed.

and serve as a useful tool to test various interesting ideas.

Learning and memory is one primary function of the neural system, which is crucial in developing behaviors to adapt to an ever-changing environment. So far, our understanding of the physiology of learning and memory is far from complete. It is now believed that learning involves synaptic plasticity, that is, changes in the structure or biochemistry of synapses that alter their effects on postsynaptic neurons. In particular, previous studies (Wise, 1996; Reynolds et al., 2001; Packard and Knowlton, 2002; Schultz et al., 2003) have demonstrated the involvement of the striatum in numerous forms of learning and memory. Such an involvement is likely based on changes in neuronal activity in the striatum during learning. The increase in task-related neuronal activity might lead to synaptic changes at striatal synapses, such as the reinforcement of synaptic strength due to a Hebbian learning rule. This mesoscopic mechanism could underlie the learning of stimuli that predicts rewards and induces the preparation of movements. Nevertheless, we still know very little about learning and memory at various developing stages of a neural network.

One of the most complicated neural networks is the human brain; it consists of one hundred billion neurons and each neuron has fifty thousand connections to others. Any attempt to simulate a network with such an enormous complexity would be almost impossible. A simpler system for computer simulations is culture samples of neural networks prepared from the cerebral cortex of embryonic rats. In this paper, we attempt to study learning-induced synchronization of a developing neural network, whose size ranges from tens to hundreds of neurons. Since we focus on the robust properties of collective neuronal dynamics which are not sensitive to details of neurons (Uery and Reid, 1999; Tresch and Kiehn, 2002; Zhigulin et al., 2003), we apply a one-dimensional map with excitable dynamics representing the neuronal activities of the network, instead of a biological model of action potential (AP) for nerve cells (Labos, 1986; Hayakawa and Sawada, 2000). In our model, each neuron integrates all the inputs from other neurons and fires whenever the membrane potential reaches a threshold. The firing dynamics of neurons can be investigated at various stages of a developing network. A detailed description of our model is given in Section 2. The advantage of this model is its capability to investigate large size neural networks using

reasonable computational efforts. Results from our simulations are consistent with recent experimental observations. However several parameters used in this model rely on experimental measurements and cannot be calculated directly from a microscopic theory. In Section 3, we present our results and discussion on the initiation of synchronization behavior of a developing neural network as the number of connections between neurons increases. We show that the time dependence of the synchronous firing frequency of neural networks predicted from this model is consistent with that observed in experiments. In addition, synaptic plasticity and enhancement effects induced by learning are also investigated for a developing network. Here “learning” refers to the Hebbian learning of neurons due to an external signal (described by Eq. (4) or Eq. (5) in Section 2), and “developing” refers to the wiring and pruning of the network depending on the activity of the cells to form specific connections (described by Eq. (1) in Section 2). Section 4 contains our main conclusions.

2. Model

We consider the firing dynamics of a developing neural network of N fixed neurons, which are randomly grafted on a substrate of size $L \times L$. These neurons are not connected to each other initially. The development of the neural network involves with two time scales: At long time scale (T_0 , in unit of hours), the network gradually builds up connections between neurons; at short time scale (τ_0 , in unit of 10 milliseconds), neurons communicate with each other through existing connections. During our simulations, the network connectivity is updated every 10^4 runs of neuronal communications. The probability of forming a synapse between two neurons is assumed to have the following power-law form:

$$p = \frac{k}{r_{ij}^\alpha}, \quad (1)$$

where r_{ij} is the distance between neurons i and j . The coefficient α implies the connection mechanism between two neurons. The connection between two neurons is random for $\alpha = 1$, since the connection probability is inversely proportional to the searching circumference for the axon. Long-distance connections are favored for $\alpha < 1$, while they are disfavored for

$\alpha > 1$. In general, the coefficient k would depend on the level of activity in the network (for example, local concentration of neurotrophins) and play roles in regulating neuronal plasticity. Here, for simplicity, we assume a constant k for the entire network at all times. Note that, although we have assumed a simple form of connection probability between two neurons, the exact connection probability is not known experimentally and is probably different for different systems. The neuronal activity is described by a one-dimensional iterative map $v(t+1) = f(v(t))$ with the following form (Hayakawa and Sawada, 2000):

$$f(v) = \begin{cases} 0 & \text{for } v < -1 \\ av & \text{for } -1 \leq v < 0.2 \\ av - 0.1 & \text{for } 0.2 \leq v < 0.85 \\ c(v-1) & \text{for } 0.85 \leq v \end{cases}, \quad (2)$$

where $v(t)$ (in arbitrary unit) is the membrane potential of neurons at time t . The coefficients $a > 0$, $b > 1$, and $0 < c \ll 1$ are constants and determine the shape of firing pulses. This map, as shown in Fig. 1(a) has an unstable fixed point at $v_u = 0.2$, above which the

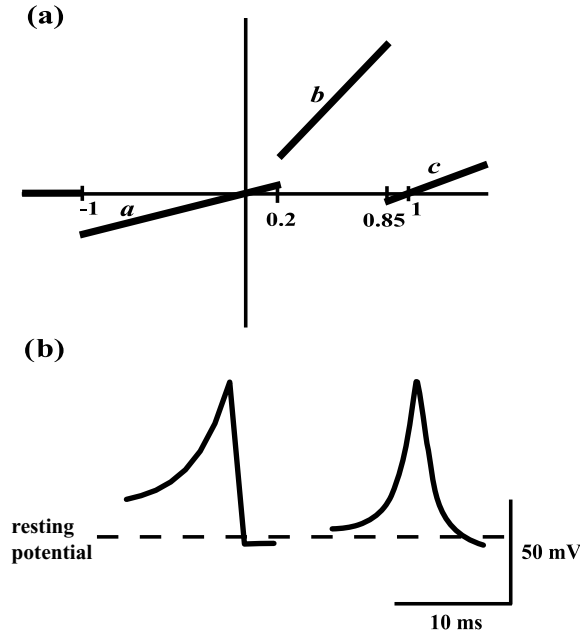


Figure 1. A simplified representation of the neuronal activity including (a) a piecewise-linear one-dimensional map $f(v)$ and (b) a comparison of the simulated AP using $f(v)$ (left) and one experimentally recorded AP (right). The coefficients a , b , and c are the slopes in each segment. The units of the short time scale t and the AP v are set to be 3 ms and 70 mV respectively in (b).

neuron will fire a single pulse, drop below its resting potential, and gradually return to normal value. Therefore this map can generate a realistic AP even though some biological details are ignored. In Fig. 1(b), we show a comparison of a computer generated AP using Eq. (2) (left) with an experimentally recorded one of CA1 pyramidal cell of rats (right) (Bikson et al., 2002). Notice that, in our model, the initial membrane potential must exceed the threshold v_u before the neuron can fire an action potential. This threshold has been observed in many experimental and theoretical studies, but it is not apparent in the recorded potential in Fig. 1(b). Following the paper of Hayakawa and Swada, we choose $a = 0.5$, $b = 1.5$, and $c = 0.04$ in our simulations.

For a partially connected and externally controlled neural network, the activity of each neuron is affected by connected neurons and an external bias. For the i -th neuron, we express its activity as

$$v_i(t+1) = f\left(v_i(t) + \sum_{j \neq i}^N w_{ij} v_j(t - \tau) + v_i^e(t)\right), \quad (3)$$

where i and j are the neuron indices, $v_i^e(t)$ is the external bias to the i -th neuron, w_{ij} is the synaptic strength from neuron j to i , and τ is the delay time. For simplicity, a constant delay time is assumed. In our simulations, a learning algorithm is also introduced to the neural network. Assuming the spike-timing-dependent synaptic plasticity (STDP) rule (Markram, 1997; Song et al., 2000; Bi and Poo, 2001), the change in the synaptic strength (Δw_{ij}) due to learning at each time step can be expressed as the following:

$$\Delta w_{ij}(\Delta t) = \begin{cases} A_+ \exp(-\Delta t/\tau_+) & \Delta t > 0 \\ -A_- \exp(\Delta t/\tau_-) & \Delta t < 0 \end{cases}, \quad (4)$$

where Δt is the time of the postsynaptic spike minus the time of the presynaptic spike. The parameters τ_+ and τ_- determine the ranges of pre-to-postsynaptic interspike intervals over which synaptic strengthening and weakening occur. A_+ and A_- , which are both positive, determine the maximum amounts of synaptic modification. Alternatively, we also consider a pure Hebbian plasticity (PHP) rule (Koch, 1999; Hayakawa and Sawada, 2000), which is expressed as:

$$\Delta w_{ij}(t) = \varepsilon v_i(t) v_j(t - \tau'), \quad (5)$$

where τ' determines the ranges of pre-to-postsynaptic interspike intervals. If the firing of postsynaptic cells lags the firing of presynaptic cells by a time τ' , the learning rule in Eq. (5) will lead to a maximal synaptic facilitation. Synaptic facilitation decreases if the firing time difference differs from τ' . Synaptic depression can occur when postsynaptic cell fires shortly before presynaptic one. Previous experiments (Markram, 1997) have demonstrated that postsynaptic APs are initiated in the axon and then propagate back into the dendritic arbor of neocortical pyramidal neurons, evoking an activity dependent dendritic Ca^{2+} influx that could be a signal to induce modifications at the dendritic synapses that were active around the time of AP initiation. Therefore the synaptic efficacy can be regulated depending on the precise timing of postsynaptic APs relative to excitatory postsynaptic potentials (EPSP). The characteristic time intervals (τ_+ and τ_-) for synaptic modifications are found to be 17 ms for facilitation and -34 ms for depression for layer 5 pyramidal neurons in somatosensory cortex (Bi and Poo, 2001). Since w_{ij} can be positive or negative, both excitatory and inhibitory synapses are allowed in our network. This simplification is convenient for simulating large size networks, but it is not realistic for neurons and synapses to switch between excitatory and inhibitory depending on activity. This problem can be easily remedied by making two populations of neurons, excitatory and inhibitory, and adjusting the synaptic strengths within these populations. In Section 3, a comparison between results from these two models will be discussed. In general, the matrix of synaptic strength is asymmetric. A change in the synaptic strength might result from remodeling of synapses in both presynaptic loci and postsynaptic terminals. Saturation of synaptic efficacy can occur after repeated potentiation, and previous experiments have shown that saturation of hippocampal LTP impairs spatial learning (Castro et al., 1989; Moser et al., 1998). In this manuscript, for simplicity, we did not introduce saturation for the synaptic efficacy since we study the simplified case that the learning due to the external signal is turned off before the synaptic efficacy saturates. We note that several stabilization procedures can terminate learning either when activity levels reach a certain threshold level (Nass and Cooper, 1975) or invoke a bound on synaptic weight strengths (Linsker, 1986). The Hebbian learning rule is believed to highly correlate with the induction of long-term potentiation (LTP), which serves as a model for learning and memory and offers the most direct link from the molecular

to the behavioral levels of analysis. The time evolution of the neural network follows Eq. (3) as well as Eq. (4) or Eq. (5) at the short time scale, while the connectivity of neurons is updated according to Eq. (1) at the time scale of hours.

3. Results and Discussion

3.1. Synchronous Firing Frequency: Simulations and Experiments

In Section 2, we have constructed a simple model of neural networks based on an experimentally observed Hebbian learning rule. Particularly, our assumptions on the synaptogenesis and the neuronal activity are very simplified. Nevertheless we show that simulation results using such a simple model are consistent with recent experimental observations (Jia et al., 2004). In the experiment, neuronal culture samples are prepared from the cerebral cortex of embryonic days 17 – 18 and observed using a fluorescence microscope. Firings of the networks are monitored by the intracellular Ca^{2+} concentration changes and recorded by an intensified CCD video camera. The time dependence of the synchronous firing frequency f of the network is observed to follow a logarithmic form: $f = f_c + f_o \ln(t/t_c)$, where f_c is the minimum firing frequency and t_c is a threshold of growing time. In our simulations, 200 neurons are randomly grafted on a square substrate of size $L = 200$ (the size of a soma is set to unity). The initial neuron states are set with an average of 0.4 and a standard deviation of 0.3. Initially, there is no connection between neurons. When synapses are formed, the initial synaptic strength has a zero average and a standard deviation of 0.04. All neurons are under a 0.1 DC bias for the learning rule in Eq. (4) or a 0.05 DC bias for the learning rule in Eq. (5). As shown in Fig. 2, our simulation results for the synchronous firing frequency of the network are consistent with experimental observations (squares). This result demonstrates that the developing rule in Eq. (1) and the learning rule in Eq. (4) or Eq. (5) together determine the synchronous firing frequency of a developing network. Nevertheless, we note that larger values of α tend to shift simulation results away from the experimental data if they are fitted to the same curve. Changing the exponent will also affect the two characteristic time scales, T_0 and τ_0 , when the simulation data are fitted to the experimental results. The short time scale, τ_0 , decreases as the exponent increases. The inset of Fig. 2 shows the

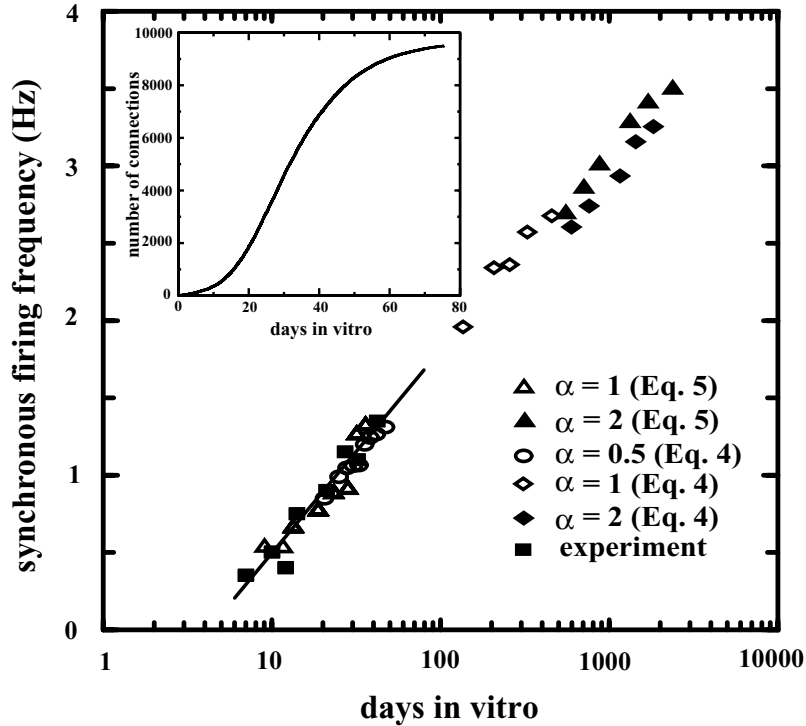


Figure 2. A comparison of results from our simulations (open triangles: $\alpha = 1$ and Eq. (5); filled triangles: $\alpha = 2$ and Eq. (5); open ovals: $\alpha = 0.5$ and Eq. (4); open diamonds: $\alpha = 1$ and Eq. (4); filled diamonds: $\alpha = 2$ and Eq. (4)) and from experiments (squares) for the time dependence of the synchronous firing frequency of neural networks. The solid line is the best fit to the experimental data. The parameter set used is $\{k = 10^{-5}, A_+ = 10^{-3}, A_- = 8 \times 10^{-4}, \tau = 3\tau_0, \tau_+ = \tau_0, \tau_- = \tau_0\}$ for the learning rule in Eq. (4), and is $\{k = 10^{-5}, \varepsilon = 5 \times 10^{-4}, \tau = \tau_0, \tau' = \tau_0\}$ for the learning rule in Eq. (5). Here the set of time scales $\{T_0, \tau_0\}$ is $\{0.18 \text{ h}, 70 \text{ ms}\}$, $\{0.6 \text{ h}, 63 \text{ ms}\}$ and $\{0.6 \text{ h}, 48 \text{ ms}\}$, for $\alpha = 0.5, 1$, and 2 respectively for the learning rule in Eq. (4), while it is $\{0.12 \text{ h}, 500 \text{ ms}\}$ and $\{0.6 \text{ h}, 125 \text{ ms}\}$ for $\alpha = 1$ and 2 respectively for the learning rule in Eq. (5). The inset shows the number of connections among neurons calculated from our simulations as a function of days in vitro for $\alpha = 1$.

time dependence of the network connectivity (number of connections, N_c) for $\alpha = 1$, which can be fitted by a logarithmic function in the range of consideration. Therefore the synchronous firing frequency increases linearly with the network connectivity. It is then clear that, as the mean connectivity of the network increases, the enhanced communications among neurons lead to an increase in the synchronous firing frequency. This conclusion is also confirmed by experimentally studying the effect of Mg^{2+} on the firing frequency and network connectivity (Jia et al., 2004).

3.2. Synchronous Activity of Neural-Networks with Different Designs

To further study this model, we consider that initially 40 isolated neurons (N) are grafted on a square substrate of size $L = 200$ with random membrane

potentials (v_i); the neuronal states v_i are chosen to have an average of 0.2 and a variance of 0.2. We choose the parameter set $\{\alpha = 1, k = 5 \times 10^{-4}, A_+ = 5 \times 10^{-4}, A_- = 5.25 \times 10^{-4}, \tau = 9\tau_0, \tau_+ = 3\tau_0, \tau_- = 3\tau_0, \tau_- = 3\tau_0\}$ for the learning rule in Eq. (4) and $\{\alpha = 1, k = 5 \times 10^{-3}, \varepsilon = 5 \times 10^{-4}, \tau = 9\tau_0, \tau' = 9\tau_0\}$ for the learning rule in Eq. (5). The initial synaptic weight between neurons is set to have a zero average and a variance of 0.03 ($w_{ij} = 0$ if neurons i and j are not connected). In addition, a quarter of neurons are externally biased by a sine wave of period $T = 50\tau_0$ and amplitude $A = 0.5$ during the first 4000 learning time steps (T_L). We note that oscillations in neural networks usually serve various physiological functions (Penttonen et al., 1999; Mikkonen et al., 2002), which is why a simpler DC drive is not utilized. After this learning phase, the network enters a so-called recall phase, in which the external signal is turned off and the learning coefficient is set to zero. The neuronal

activity in this recall phase is investigated by averaging results from 300 different runs.

During the learning phase, frequent firing is observed near the peak of the external signal for biased neurons. For a network with sufficient connections, the

firing activity is gradually seen for non-biased neurons, although their neuronal states might have different phase and/or frequency. At the steady state of the recall phase, for an appropriate learning coefficient, the neuronal activity persists in the absence of the

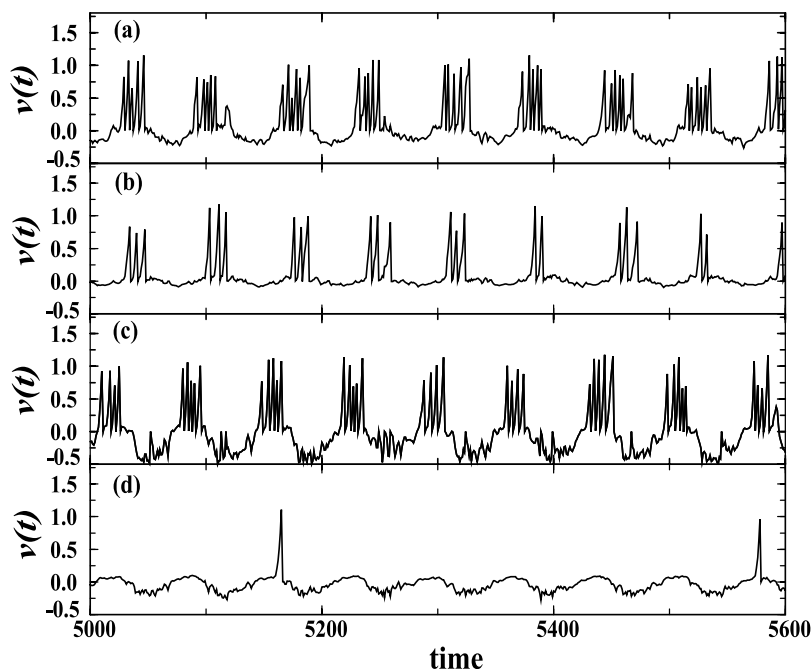


Figure 3. Neuronal activities of various neurons in a partially connected network after learning induced by an external signal, including (a) synchronized firing of a biased neuron, (b) synchronized firing of a non-biased neuron, (c) out-of-phase firing of a non-biased neuron, and (d) random firing of a non-biased neuron. Here the learning rule in Eq. (5) is adopted.

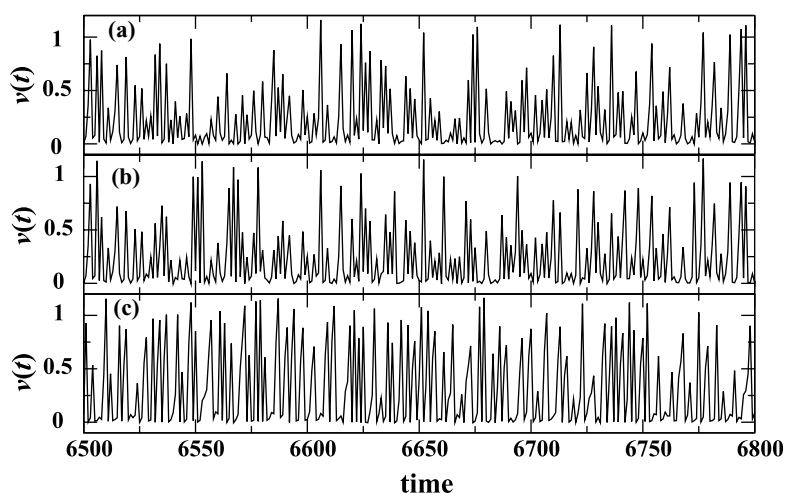


Figure 4. Neuronal activities of various neurons in a partially connected network after learning induced by an external signal, including (a) synchronized firing of a biased neuron, (b) synchronized firing of a non-biased neuron, and (c) out-of-phase firing of a non-biased neuron. Here the learning rule in Eq. (4) is adopted.

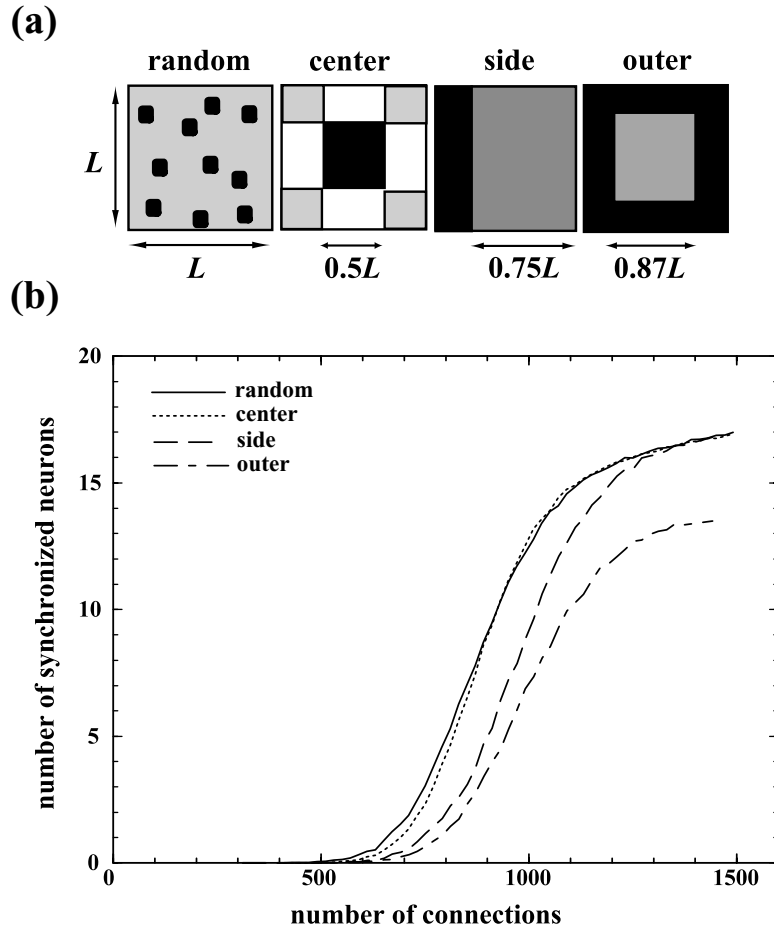


Figure 5. Investigation of the synchronized firing behavior for various neural networks with different designed patterns: (a) four different designed patterns studied, and (b) the dependence of the number of synchronized neurons on the number of connections between neurons in the network for the learning rule in Eq. (5). In (a) biased neurons are grafted in the black regions, while non-biased neurons are grafted in the grey regions. To smoothen those curves in (b) for a better presentation of our results, each data point (at N_c) in the curves is an average within the range ($N_c, N_c + 20$).

external signal. Figure 3 shows various neuronal states in the recall phase for the learning rule of Eq. (5). Synchronized firing is observed for both biased (a) and non-biased (b) neurons. For non-biased neurons, we also observe out-of-phase firing (c) and random firing (d). Figure 4 shows various neuronal states in the recall phase for the learning rule of Eq. (4), which exhibits synchronized firing for biased (a) and nonbiased (b) neurons as well as out-of-phase firing for nonbiased neurons (c). However, random firing is not observed in this case. The mechanism leading to oscillations is due to the delayed connections (Shayer and Campbell, 2000). In the limit of zero delay, no oscillation is observed. In fact, the network without delays becomes inactive after the removal of the ex-

ternal signal. Our simulations show a robust behavior for the reproduction of stimuli over a wide range of parameters ε and T_L for the learning rule in Eq. (5), which is not observed for the learning rule in Eq. (4).

Synchronous activity among individual neurons is a robust phenomenon in many regions of the brain (Usrey and Reid, 1999; Tresch and Kiehn, 2002; Zhigulin et al., 2003). To study how synchronization occurs as a neural network develops, in Figs. 5 and 6, we calculate the average number of synchronous neurons in the recall phase for a network at various developing stages. Here two neurons (i and j) are defined to be synchronized if both neurons are active and their time correlation ($C_{ij} \equiv \langle [v_i(t) - \langle v_i(t) \rangle][v_j(t) - \langle v_j(t) \rangle] \rangle$), where angular brackets denote a time average) is greater than

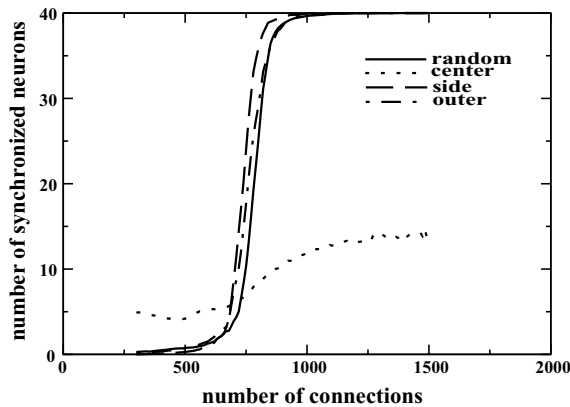


Figure 6. The dependence of the number of synchronized neurons on the number of connections between neurons in the network for the learning rule in Eq. (4). To smoothen those curves in (b) for a better presentation of our results, each data point (at N_c) in the curves is an average within the range $(N_c, N_c + 50)$.

0.2. In addition, we are also interested in the synchronization behavior of various networks with different designed patterns. Such a study would be useful in controlling the physical properties of a neural network by a specifically designed pattern. As schematically illustrated in Fig. 5(a), four networks with different patterns are studied: “random” denotes a randomly grafted network with randomly chosen biased neurons, “center” denotes a network in which the biased neurons are located at the center region and non-biased ones are grafted at four corner regions, “side” denotes a randomly grafted network in which biased neurons are located at one side, and “outer” denotes a randomly grafted network in which the biased neurons are located at the outer regions. The number of synchronized neurons is calculated at various developing stages for these four networks using the learning rule of Eq. (5), as shown in Fig. 5(b). It is shown that there is no synchronization if the N_c is less than 600, while the number of synchronous neurons reaches a plateau at around 1300 connections. For a network with 40 neurons, the maximal number of connections between

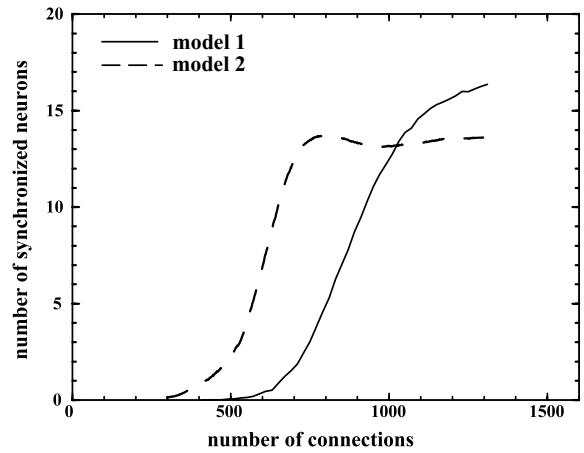


Figure 7. The dependence of the number of synchronized neurons on the number of network connections for the learning rule in Eq. (5). In model 1, synapses can switch between excitatory and inhibitory depending on their activity. In model 2, the switching between excitatory synapses and inhibitory synapses is not allowed.

neurons is 1560. This finding implies that synchronization of neurons occurs in the early stage of a developing neural network, but matures at a late stage of development. Note that the percolation transition of our neural networks (in which case a path among neurons is built from one side of the substrate to the opposite side) occurs at about 40 connections. The synchronization of networks occurs at a stage much later than that of percolation of networks. We also note that all four patterns show a continuous phase transition in the synchronization of neurons as the network develops. Furthermore, we compare the synchronization behavior of these four patterns. In Fig. 5(b), the time sequence for the initiation of synchronization is followed by “random”, “center”, “side”, and “outer”. The two patterns denoted by “random” and “center” initiate synchronization at 700 connections and are quite similar in their synchronization behavior, but “side” and “outer” initiate synchronization at around 800 connections. We note that similar results are also obtained when synapses of very weak efficacy (after learning)

Table 1. The average distance and number of connections between biased neurons and others for four neural networks with different designed patterns.

Pattern	Random		Center		Side		Outer	
Distance	104.6		111.8		122.7		128.8	
Connections	17.6	20.1	19.0	21.8	16.4	18.8	15.0	17.4
	$N_c = 700$	$N_c = 800$						

are removed. In fact, the critical N_c to initiate synchronization is smaller in this case. Although several factors could affect the synchronization behavior of a network, we suspect that synchronization is mainly affected by those connections to the biased neurons. As shown in Table 1, the average distance between biased neurons and others for these four networks is consistent with the above result in Fig. 5(b). Since the connection probability between neurons is inversely proportional to the distance between neurons, the average number of connections to the biased neurons follows a similar trend for various values of N_c . The only exception is the pattern denoted by “center”, in which over 30% connections are between biased neurons (the rate of connections between biased neurons are about 20% for the “random” pattern). Thus the data in Table 1 support our conjecture on the synchronization of networks. However, when the number of connections to the biased neurons is small, the maximal number of synchronized neurons is also reduced as observed in the pattern denoted by “outer”.

Figure 6 shows the relation between the number of synchronized neurons and the number of network connections for the learning rule in Eq. (4). It is clearly seen that the synchronization behavior of the “center” network differs drastically from that of the other three networks. For the “center” network, biased neurons are located in the central area and thus the network establishes many connections between active biased neurons at the early developing stage. For this reason, there exists finite number of synchronized neurons in the “center” network at the early developing stage ($N_c < 600$), but there are almost no synchronized neurons for the other three networks. As the networks further evolve, more non-biased neurons become active in the other three networks, and the number of synchronized neurons increases suddenly at $N_c \sim 700$ and reaches 40. On the other hand, for the “center” network, the connections between nonbiased neurons and biased neurons are relatively rare such that many nonbiased neurons are not excited by biased neurons. In this case, the saturated number of synchronized neurons in the “center” network is only a third of that in the other three networks.

By comparing Figs. 5 and 6, we find some major differences between our learning rules in Eqs. (4) and (5). The STDP model in Eq. (4) tends to give a quasi-first order transition for the synchronizing behavior of most networks, while the PHP model leads to a second order transition for the synchronizing behavior of all four

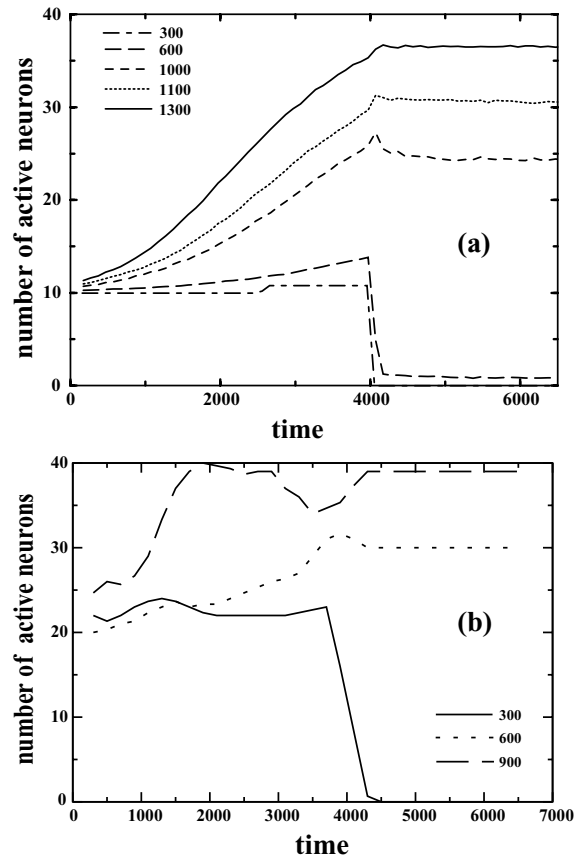


Figure 8. The time evolution of the number of active neurons for the “random” neural network of various numbers of neuronal connections for the PHP model (a) or for the STDP model (b). The external drive is removed at $t = 4000$.

networks. It is clear that the learning rule in Eq. (4) has a much greater learning effect than that in Eq. (5). We have also tried to reduce the learning coefficient in the STDP model and find no network activity for smaller learning coefficients. This also demonstrates the first order characteristic (all or none) of the STDP model.

In our simulations, an initial Gaussian distribution of synaptic weight w_{ij} is used. For simplicity, we deliberately do not distinguish excitatory and inhibitory neurons for the learning rule in Eq. (5) (model 1). This assumption is not realistic since neurons and synapses cannot switch between excitatory and inhibitory depending on activity. Here we consider another model (model 2) for the learning rule in Eq. (5), where switching between excitatory and inhibitory is not allowed for neurons. A comparison in the synchronized activity of the network of these two models is given in Fig. 7. In model 2, all biased neurons and one third of unbiased

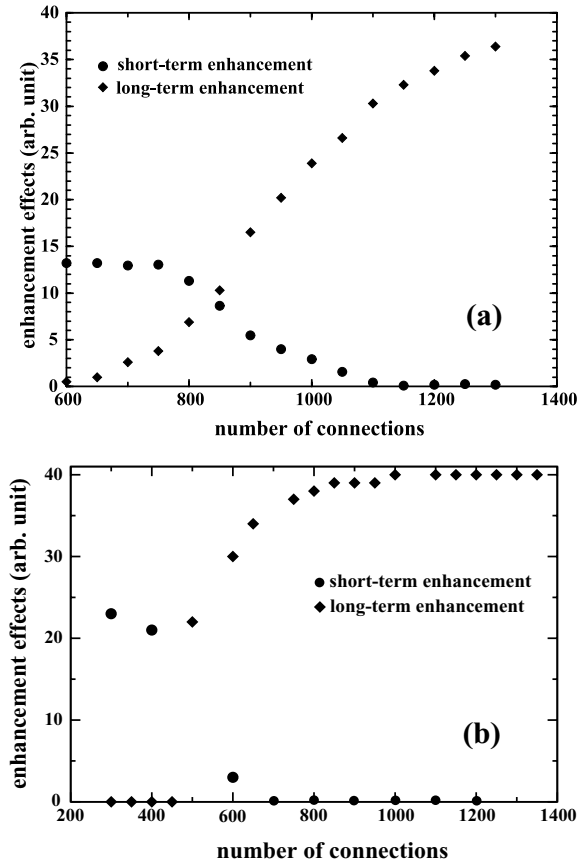


Figure 9. Enhancement effects induced by learning as a function of the number of neuronal connections for the PHP model (a) or for the STDP model (b). Long-term enhancement is favored for networks with a large number of connections, while short-term enhancement dominates for networks with few connections.

neurons are excitatory. Both models show a continuous increase in the number of synchronized neurons (N_s) as the network develops, and N_s saturates at large numbers of network connections. However, the maximal value of N_s and the critical value of N_c to initiate synchronization are both smaller in model 2. From our simulations, we find that the maximal value of N_s and the critical value of N_c depend on the number of inhibitory neurons. In model 1, some inhibitory synapses switch to be excitatory due to learning, which effectively reduces the percentage of inhibitory synapses of the network. Other than that, both models seem to give consistent results.

3.3. Short- and Long-Term Enhancement Effects

The plasticity of our networks enforced by Eq. (4) or Eq. (5) is contributed from active neurons rather than

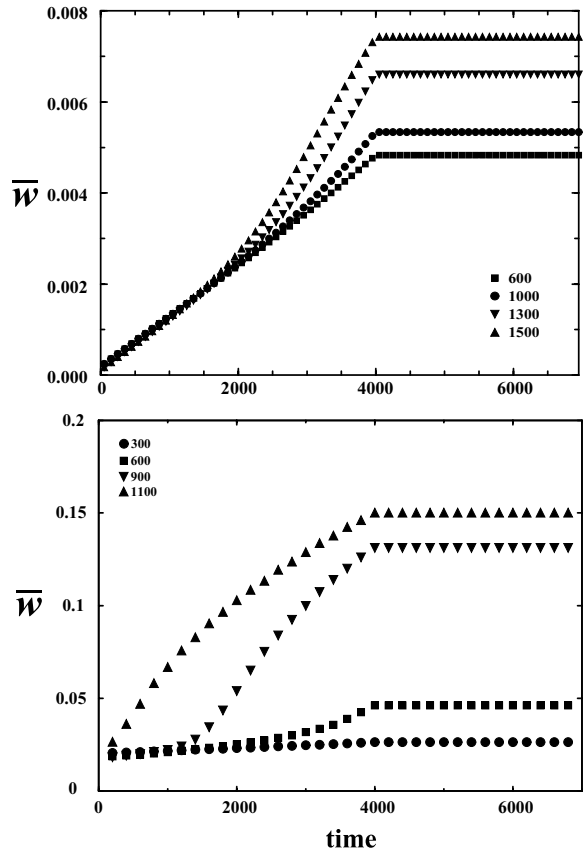


Figure 10. The time evolution of the average synaptic strength for the PHP model (a) or for the STDP model (b). Both the external signal and the learning coefficient are set to zero at time = 4000.

silent neurons. In Fig. 8, we investigate the number of active neurons of a “random” network with various numbers of connections for the PHP model (a) or for the STDP model (b). Here a neuron is defined to be active if it fires at least once within a period of T . In the presence of an external signal, the number of active neurons of the network increases with time of learning. For a network with more connections, more neurons become active at the end of the learning phase. After the external signal is removed (in the recall phase), all neurons become silent rapidly if the network has less than 600 connections, as shown in Fig. 8(a). In Fig. 8(b), the network becomes silent only for $N_c \leq 300$. It is observed that the number of active neurons overshoots at the end of the learning phase for $N_c \leq 1100$ in Fig. 8(a) and for $N_c \leq 600$ in Fig. 8(b). Clearly the increase of active neurons in the learning phase includes a short-term enhancement (which rapidly diminishes within seconds after switching off the external signal) and a

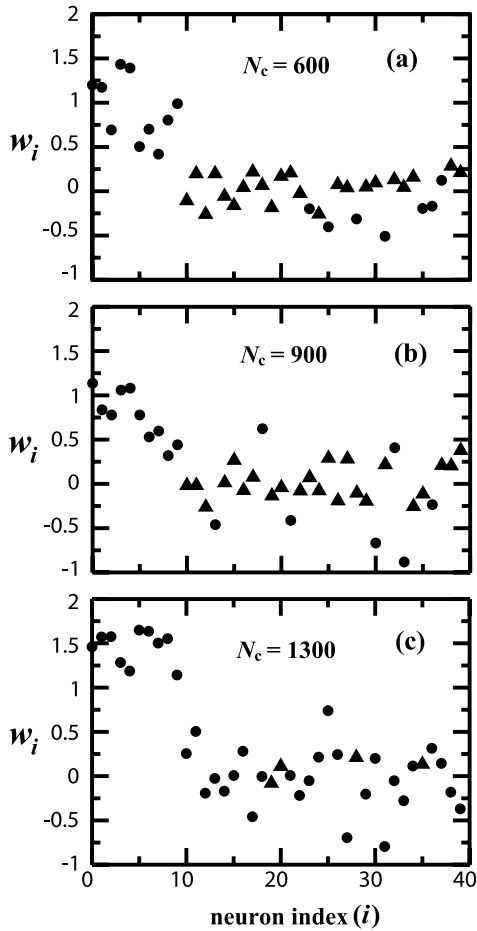


Figure 11. The synaptic strength of individual neurons for networks of $N_c = 600, 900,$ and 1300 using the learning rule in Eq. (5). Circles represent active neurons, and triangles represent silent neurons.

long-term enhancement (which lasts for much longer than seconds). Here we define the number of active neurons in the learning phase as the enhancement. This enhancement is related to the average synaptic weight of the network. The characteristic decay time of the short-term enhancement in our simulations is comparable with that of augmentation (Koch, 1999). It has been postulated that the long-term enhancement could result from structural remodeling of synapses or formation of new synaptic contacts (Buchs and Muller, 1996; Engert and Bonhoeffer, 1999; Toni et al., 1999). This postulate is consistent with the results of our simulations.

In Fig. 9, we plot both the short-term enhancement and the long-term enhancement as a function of network connections. A large increase rate of active neu-

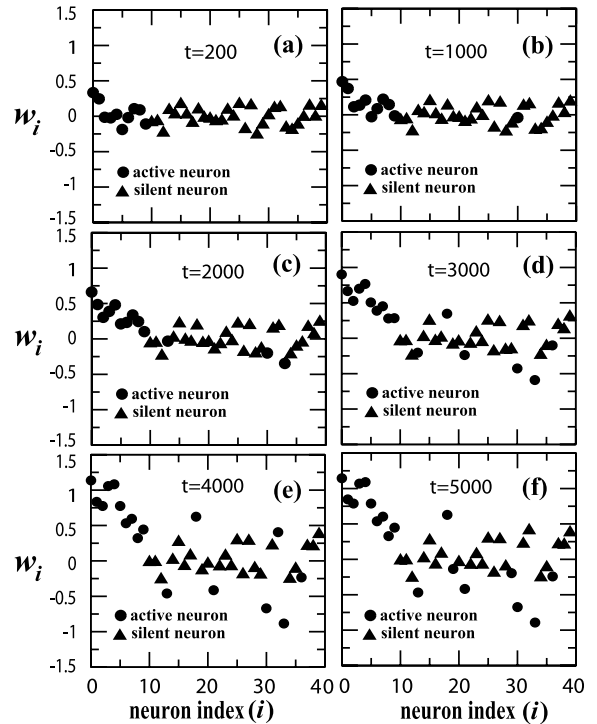


Figure 12. The synaptic strength of individual neurons at different times for a network of $N_c = 900$ using the learning rule in Eq. (5). Circles represent active neurons, and triangles represent silent neurons.

rons is found for networks with 750–1100 connections for the learning rule in Eq. (5) as shown from Fig. 9(a), which suggests that the most crucial developing period for learning occurs at the mid stage of development. For an all-to-all coupled network, almost all neurons are active. Approximately we can divide the development of a neural network into three stages, including the early stage ($N_c < 750$), the mid stage ($750 < N_c < 1100$), and the late stage ($1100 < N_c$). Similar behaviors are also observed for the learning rule in Eq. (4) as shown from Fig. 9(b). However, as we noted in the previous sub-section, the STDP in Eq. (4) tends to give a quasi-first order transition, instead of a second order transition. The growth in the long-term enhancement in STDP is much faster and occurs earlier than that in PHP. It is suggested from Fig. 9 that short-term enhancement dominates the learning effect for an infant network. Thus we believe that long-term enhancements can be initiated only after the number of network connections exceeds a threshold value. We note that both the developing rule in Eq. (1) and the learning rule in Eq. (4) or Eq. (5) are important for these enhancement effects. In particular, for the long-term enhancement to

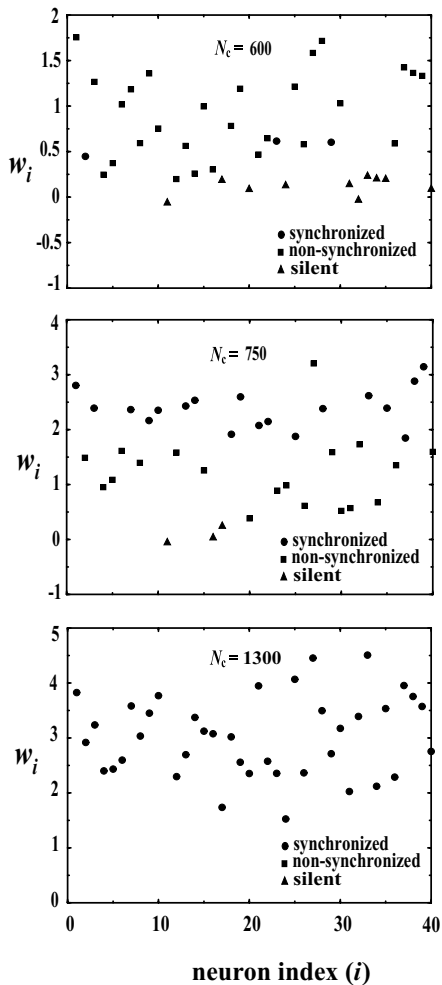


Figure 13. The synaptic strength of individual neurons for networks of $N_c = 600, 750$, and 1300 using the learning rule in Eq. (4). Circles represent synchronized neurons, squares represent non-synchronized neurons, and triangles represent silent neurons.

occur, neurons in the network must establish enough connections and the synaptic strength of these connections must be enhanced through learning.

3.4. Synaptic Plasticity of Neural-Networks

To further investigate the synaptic plasticity of our networks, we calculate the average synaptic strength of the random network as a function of time for various numbers of connections, as shown in Fig. 10. Here we define the average synaptic strength of the network as $\bar{w} = (\sum_{i,j=1}^N w_{ij})/N_c$ and the integrated synaptic strength of i -th neuron as $w_i = \sum_j w_{ij}$. For the PHP

model, as shown in Fig. 10(a), the growth curves of the average synaptic strength of the network in the learning phase follow a simple power law. The exponents of these curves are 1.07, 1.21, 1.53, and 1.57 for networks with 600, 1000, 1300, and 1500 connections, respectively. The early stage of the network is characterized by a nearly linear synaptic plasticity, while the growth of the average synaptic strength in the late stage has an exponent greater than 1.5. Typically, saturation of synaptic efficacy can occur after repeated potentiation. Therefore, a cutoff for the synaptic weight should be introduced in the PHP model to avoid divergence in synaptic weight. For the STDP model, as shown in Fig. 10(b), the growth curves of the average synaptic strength of the network in the learning phase are very different from those in Fig. 10(a). These growth curves increase rapidly with time initially, but eventually reach a threshold at longer times.

In Fig. 11, for the learning rule in Eq. (5), we show the synaptic strength of individual neurons at the end of the learning phase in a typical simulation for $N_c = 600, 900$, and 1300 . The first ten neurons in all networks are biased and thus have unusual high synaptic strengths. On the average, active neurons tend to have a greater synaptic strength (in absolute value) than silent neurons. However, some active neurons can have rather small absolute synaptic strength, particularly for networks with a large number of neuronal connections due to Eq. (3). The time evolution of the distribution of synaptic strength of individual neurons for a network with 900 connections for the PHP model is given in Fig. 12. The first ten neurons are activated initially due to the external signal (a). As time evolves, silent neurons can be activated through their connections with biased neurons, even though their absolute synaptic strengths are small (b). It is observed that the absolute synaptic strength of active neurons increases much more rapidly than that of silent neurons (c–f). For the learning rule in Eq. (4), in Fig. 13, we show the synaptic strength of individual neurons at the end of the learning phase in a typical simulation for $N_c = 600, 750$, and 1300 . It is also found that active neurons usually have a greater synaptic strength (in absolute value) than silent neurons. Moreover, we notice that the synaptic weights of synchronized neurons are about the same for $N_c = 600$ and 750 . For $N_c = 1300$, all neurons become synchronized but their synaptic weights are very different from each other. The time evolution of the distribution of synaptic strength of individual neurons for a network with 750 connections for the STDP model is

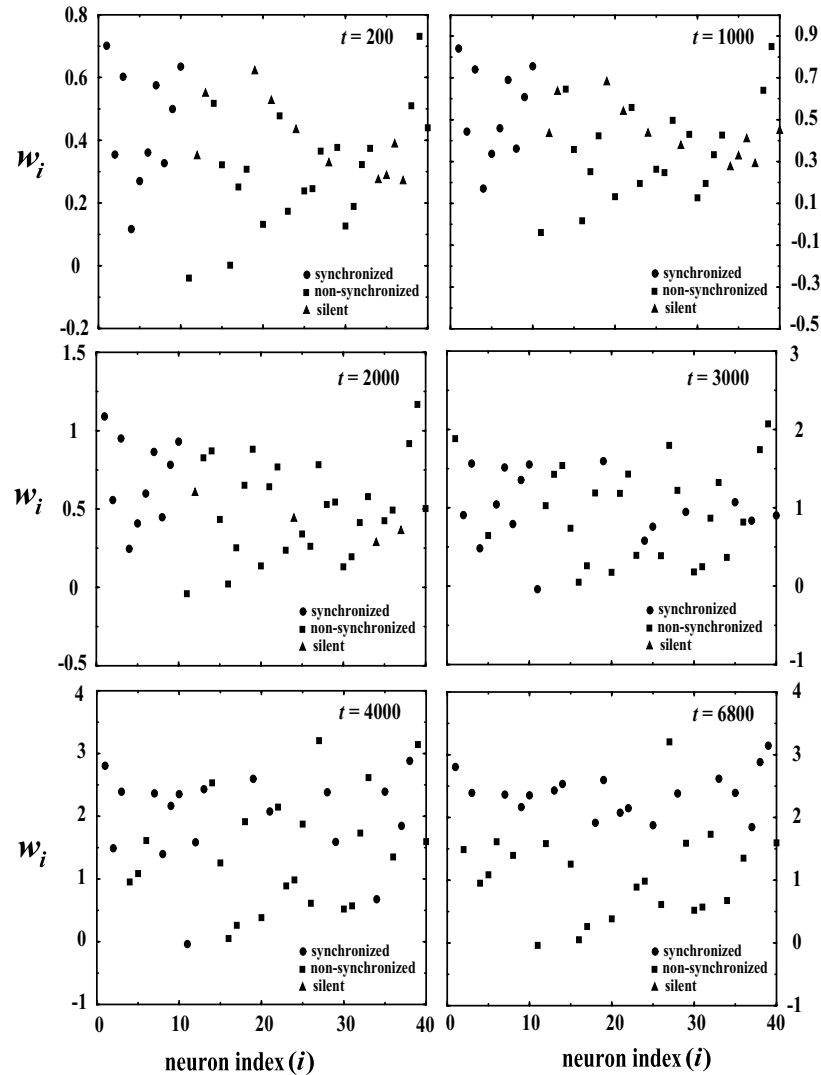


Figure 14. The synaptic strength of individual neurons at different times for a network of $N_c = 750$ using the learning rule in Eq. (4). Circles represent active neurons, squares represent non-synchronized neurons, and triangles represent silent neurons.

given in Fig. 14. The first ten neurons are active and synchronized due to the external signal at $t = 200$. As time evolves, more silent neurons are activated due to their connections to the biased neurons. At $t = 2000$, many silent neurons become active but remain non-synchronized. The number of synchronized neurons starts to increase after $t = 3000$ and reaches a plateau in the learning phase ($t > 4000$).

4. Conclusions

In conclusion, we have applied a pulse-coupled neural network model to study the synchronization

behavior and synaptic plasticity of a developing neural network by considering two types of Hebbian learning rules. The time dependence of the synchronous firing frequency of neural networks predicted from our models is shown to be consistent with that observed in experiments. For the PHP model, the number of synchronized neurons after the removal of the external signal shows a continuous transition as the number of network connections increases. Nevertheless, for the STDP model, the number of synchronized neurons shows a quasi-first order transition as the number of network connections increases. We find that the number of connections to biased neurons plays an

important role in inducing the synchronization of neurons and affecting the fraction of synchronized neurons, after analyzing four networks with different designed patterns. The synaptic plasticity of the network is also very different at various developing stages. After learning, we only observe short-term enhancement effects for a network at its early developing stage. As the network further evolves, both short-term and long-term effects are observed. For the largest increasing rate of active neurons to occur, the network connection ratio is about 50% in the PHP model and is about 30% in the STDP model. We consider this stage as the most effective learning period. For a globally coupled neural network, long-term enhancement effects are favored.

Acknowledgments

We thank C.K. Chan and K.T. Lu for stimulating discussions. This work is supported, in part, by the National Science Council of Taiwan under grant no. NSC 93-2112-M-003-004 and by National Taiwan Normal University under Grant No. ORD92-3.

References

- Ahmari SE, Buchanan J, Smith SJ (2000) Assembly of presynaptic active zones from cytoplasmic transport packets. *Nature Neurosci.* 3: 445–451.
- Ben-Ari Y (2001) Developing networks play a similar melody. *Trends Neurosci.* 24: 353–360.
- Ben-Ari Y, Cherubini E, Corradetti R, Gaiarsa JL (1989) Giant synaptic potentials in immature rat CA3 hippocampal neurons. *J. Physiol. (Lond)* 416: 303–325.
- Bi B, Poo M (2001) Synaptic modification by correlated activity: Hebb's postulate revisited. *Annu. Rev. Neurosci.* 24: 139–166.
- Bikson M, Bihi RID, Vreugdenhil M, Köhling R, Fox JE, Jefferys JGR (2002) Quinine suppresses extracellular potassium transients and ictal epileptiform activity without decreasing neuronal excitability in vitro. *Neurosci.* 115: 251–261.
- Buchs PA, Muller D (1996) Induction of long-term potentiation is associated with major ultrastructural changes of activated synapses. *Proc. Natl. Acad. Sci. USA* 93: 8040–8045.
- Castro CA, Silbert LH, McNaughton BL, Barnes CA (1989) Recovery of spatial learning deficits after decay of electrically induced synaptic enhancement in the hippocampus. *Nature* 342: 545–548.
- Engert F, Bonhoeffer T (1999) Dendritic spine changes associated with hippocampal long-term synaptic plasticity. *Nature* 399: 66–70.
- Hayakawa Y, Sawada Y (2000) Learning-induced synchronization of a globally coupled excitable map system. *Phy. Rev. E Stat. Nonlin. Soft Matter Phys.* 61: 5091–5097.
- Jia LC, Sano M, Lai PY, Chan CK (2004) Connectivities and synchronous firing in cortical neuronal networks. *Phys. Rev. Lett.* 93: 088101.
- Jontes JD, Buchanan J, Smith SJ (2000) Growth cone and dendrite dynamics in zebrafish embryos: early events in synaptogenesis imaged in vivo. *Nature Neurosci.* 3: 231–237.
- Koch C (1999) *Biophysics of Computation*. Oxford University Press, New York, pp. 308–329.
- Labos E (1986) Chaos and neural networks. In: Degn H, Holden AV, Olsen LF, eds. *Chaos in Biological Systems*. Plenum Press, New York, pp. 195–206.
- Linsker R (1986) From basic network principles to neural architecture: Emergence of spatial-opponent cells. *Proc. Natl. Acad. Sci. USA* 83: 7508–7512.
- Markram H, Lubke J, Frostscher M, Sakmann B (1997) Regulation of synaptic efficacy by coincidence of postsynaptic APs and EPSPs. *Science* 275: 213–215.
- Mikkonen JE, Grnfors T, Chrobak JJ, Penttonen M (2002) Hippocampus retains the periodicity of gamma stimulation in vivo. *J. Neurophysiol.* 88: 2349–2354.
- Moser EI, Krobot KA, Moser MB, Morris RGM (1998) Impaired Spatial Learning after Saturation of Long-Term Potentiation. *Science* 281: 2038–2042.
- Nass MN, Cooper LN (1975) A theory for the development of feature detecting cells in visual cortex. *Biol. Cybern.* 19: 1–18.
- Packard MG, Knowlton BJ (2002) Learning and memory functions of the basal ganglia. *Annu. Rev. Neurosci.* 25: 563–593.
- Penttonen M, Nurminen N, Miettinen R, Sirvio J, Henze DA, Csicsvari J, Buzsaki G (1999) Ultra-slow oscillation (0.025 Hz) triggers hippocampal afterdischarges in Wistar rats. *Neurosci.* 94: 735–743.
- Reynolds JNJ, Hyland BI, Wickens JR (2001) A cellular mechanism of reward-related learning. *Nature* 413: 67–70.
- Schultz W, Tremblay L, Hollerman JR (2003) Changes in behavior-related neuronal activity in the striatum during learning. *Trends Neurosci.* 26: 321–328.
- Shayer LP, Campbell SA (2000) Stability, bifurcation, and multistability in a system of two coupled neurons with multiple time delays. *SIAM J. Appl. Math.* 61: 673–700.
- Song S, Miller KD, Abbott LF (2000) Competitive Hebbian learning through spike-timing-dependent synaptic plasticity. *Nature Neurosci.* 3: 919–926.
- Toni N, Buchs P-A, Nikonenko I, Bron CR, Muller D (1999) LTP promotes formation of multiple spine synapses between a single axon terminal and a dendrite. *Nature* 402: 421–425.
- Tresch MC, Kiehn O (2002) Synchronization of motor neurons during locomotion in the neonatal rat: Predictors and mechanisms. *J. Neurosci.* 22: 9997–10008.
- Tyzio R, Represa A, Jorquera I, Ben-Ari Y, Gozlan H, Aniksztejn L (1999) The establishment of GABAergic and glutamatergic synapses on CA1 pyramidal neurons is sequential and correlates with the development of the apical dendrite. *J. Neurosci.* 19: 10372–10382.
- Usrey WM, Reid RC (1999) Synchronous activity in the visual system. *Annu. Rev. Physiol.* 61: 435–456.
- Wise SP (1996) The role of the basal ganglia in procedural memory. *Semin. Neurosci.* 8: 39–46.
- Zhigulin VP, Rabinovich MI, Huerta R, Abarbanel HDI (2003) Robustness and enhancement of neural synchronization by activity-dependent coupling. *Phys. Rev. E* 67: 021901.